THERMAL DAMAGE IN COMPOSITE WING BOXES.

G. La Delfa, V. Urso-Miano and A. G. Gibson
NewRail, School of Mechanical & System Engineering, Newcastle University
Newcastle upon Tyne, NE1 7RU, UK
Gaetano.La-Delfa@ncl.ac.uk

SUMMARY

This paper aims to evaluate a thermal damage assessment technique and predict the damage in composite wing box structures. A priority in the aerospace industry is the need to generate detectable methods to determine damage.

Keywords: composite structures, aerospace, fire performance, mechanical property, modelling.

ABSTRACT

Delamination damage occurs in CFRP as a result of fire exposure, followed by extensive resin decomposition and charring. The initial delaminations are detectable using portable ultrasonic equipment and appear to coincide with the onset of resin decomposition, as measured by TGA. However, further work is needed to determine the exact temperature for permanent damage. The spread of delaminations through the structure correlates with a reduction in compressive strength which can be described using the 'two layer' model. Temperature dependent thermal properties, including anisotropic values of thermal conductivity, enabled the 3-D temperature field to be modelled using an FE package. The high in-plane thermal conductivity of CFRP can result in indirect thermal damage in regions adjacent to the zone of fire exposure.

INTRODUCTION

This paper aims to evaluate the possibility of using conventional portable ultrasonic NDE equipment for thermal damage assessment in composite wing box structures following incidents such as an engine fire. While there have been a several of studies on the fire response of other types of composite material, including (1-8), there have been fewer relating to the performance of aerospace structures (9-11).

In the present study experiments were carried out on samples of wing box laminate, which were subjected to a local heat flux for different periods of time. Two heat flux levels were chosen, 185 kWm^{-2} and 75 kWm^{-2}. The highest might occur in a severe hydrocarbon-fuelled fire, such as from a large crash landing fuel spillage. This heat flux level is sometimes employed in tests on fuselage components. 75 kWm^{-2} represents a less severe, though still serious, fuel-related event.

Carbon fibre composites show greater in-plane thermal conductivity than glass fibre ones. This could lead to thermal damage in locations remote from the fire exposure site, so it was decided to devise a test to assess this effect as well as the results of direct fire exposure. The procedure used involved exposing 100mm square, 9mm thick CFRP

specimens to heat flux, over a well-defined 40mm diameter circular region, defined by a heat resistant calcium silicate mask, as in Figure 1. The heat flux was provided by a calibrated propane burner, as shown. The sample rear face was left open to air cooling and the front and rear face temperatures were measured with thermocouples.

Until recently, modelling of composite fire response has been largely based on the Henderson Equation (1, 2), which is a modified version of Laplace's unsteady-state heat conduction equation. Additional terms are required to account for the effect of the resin decomposition, which is an endothermic process, and the flow of decomposition gases through the partially decomposed laminate. This relationship has been successfully used to model the fire response of composite structures when the heat flow can be approximated to one-dimensional. However, the additional terms, especially the gas flow term, render the model difficult to apply in two or three dimensions and inconvenient to use in conjunction with commercial FE packages. It has been proposed, therefore, that the Henderson model be simplified in two ways, to avoid these problems (3). First, it is often possible to ignore the effect of the gas flow term, especially in composites such as CFRP which have a high fibre volume fraction. Secondly, the resin decomposition effect can be modelled, in a manner similar to a phase change, by incorporating it into an 'effective' temperature-dependent specific heat (3). This, in turn, can be used to calculate a temperature-dependent 'apparent thermal diffusivity'. Making these two modifications reduces the problem to the solution of Laplace's equation with a temperature-dependent thermal diffusivity term, so

$$\dot{T} = \frac{1}{\rho(T)C_P(T)}\left(k_1\frac{\partial^2 T}{\partial x^2} + k_2\frac{\partial^2 T}{\partial y^2} + k_3\frac{\partial^2 T}{\partial z^2}\right) = \alpha_1\frac{\partial^2 T}{\partial x^2} + \alpha_2\frac{\partial^2 T}{\partial y^2} + \alpha_3\frac{\partial^2 T}{\partial z^2}$$

This approach was used in the present work, in connection with the ANSYS FE package, to model the three-dimensional heat flow in the test samples.

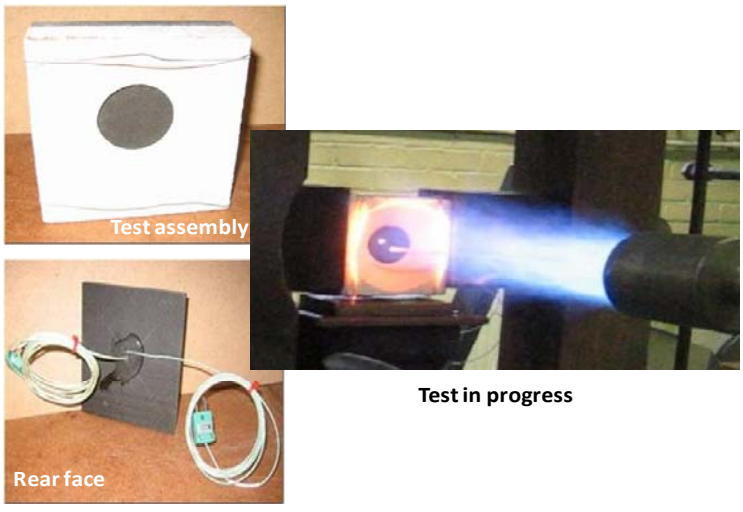

Figure 1. Fire exposure procedure showing a laminate sample with the calcium silicate mask in place and rear face thermocouple, and a fire exposure test in progress.

EXPERIMENTAL

The samples were 100 mm square, 9 mm plates of Hexcel M21/T800 CFRP, with a distributed ply content of 0°(4/9)/+45°(2/9)/-45°(2/9)/90°(1/9) and 0.63 fibre volume fraction. The experimental set-up for the fire exposure tests is shown in Figure 1, the propane burner heat flux being applied to a 40 mm diameter circular region of the laminate surface, defined by a heat-resisting calcium silicate mask. The purpose of this arrangement was to investigate the extent to which the material beneath the masked region would be influenced by heat conduction within the plane of the laminate. The burner heat flux was previously calibrated from the temperature rise in a 6 kg insulated copper block with an exposed surface of known absorptivity. The burner-specimen distance was 350 mm, the gas pressure being adjusted to give the desired heat flux values of 75 and 185 kWm^{-2}. Specimens were exposed for 30, 60, 120 and 240 seconds and allowed to cool.

The fire damage was characterised with a Sonatest RapidScan2 portable time-of-flight ultrasound scanner, with a wheel probe and phased array of 64 piezo-composite elements. This was applied to the unexposed side of the laminate, enabling lateral and through-thickness damage to be determined. In addition, optical microscopy of prepared surfaces was carried out and the residual in-plane compressive strength was measured according to ASTM D7137.

THERMAL MODELLING

In modelling the behaviour of composites exposed to fire it is necessary to take account of the thermal property changes that occur as a result of heating. The most significant effect is resin decomposition, which absorbs a significant quantity of heat and results in changes to other properties, especially thermal conductivity. Temperature-dependent values of density, specific heat and thermal conductivity were used, as shown in Figure 2. The density was derived directly from TGA data on the composite at 25 °C.min^{-1}. Most of the resin decomposition occurred in the range 350-450 °C. The Arrhenius model was not used, which resulted in some simplification. While this is conceded to result in a small error, the effect of the approximation is relatively small.

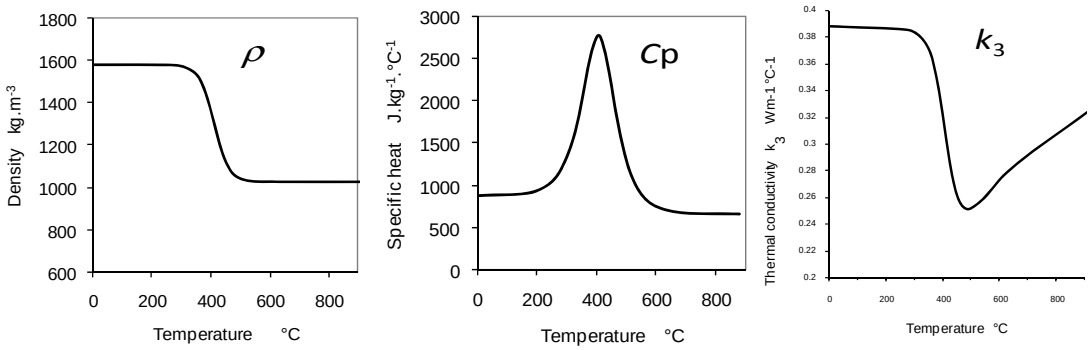

Figure 2. Temperature-dependent values of density, specific heat and through-thickness conductivity as a function of temperature.

The specific heat curve reflects the values at low temperature for the virgin laminate and high temperature for the decomposed laminate, which is mainly carbon fibre. The

endothermic effect of the resin decomposition has been added to allow for this, the area of the peak corresponding to the heat of decomposition.
Finally, over the same region, the thermal conductivity changes from that of the virgin laminate to that of the decomposed material. The conductivity is the only quantity that is a tensor, rather than a scalar. Only k_3, the through-thickness direction conductivity is shown here. This is an order of magnitude lower than the in-plane values, reflecting the low transverse-direction conductivity of the carbon fibres as well as the low conductivity of the epoxy resin. The three room temperature values of thermal diffusivity of the laminate, α_1, a_2 and α_3, were determined by simple thermal step-change measurements on laminate samples, giving values of 1.3 x 10^{-6} m^2s^{-1}, 8.1 x 10^{-7} m^2s^{-1} and 2.8 x 10^{-7} m^2s^{-1}, respectively. Using the values of specific heat and density shown in Figure 2 the thermal diffusivities were converted into thermal conductivities. The in-plane conductivity values, k_1 and k_2 are largely dominated by the relatively high fibre-direction conductivity of the carbon, so they are unlikely to change greatly as a result of the resin decomposition. It was assumed, therefore, that the in-plane conductivities were constant and equal to the room temperature values. Finally, the in-plane thermal diffusivities shown in Figure 3 were calculated. The property values shown in Figures 2 and 3 were used with the ANSYS FE model.

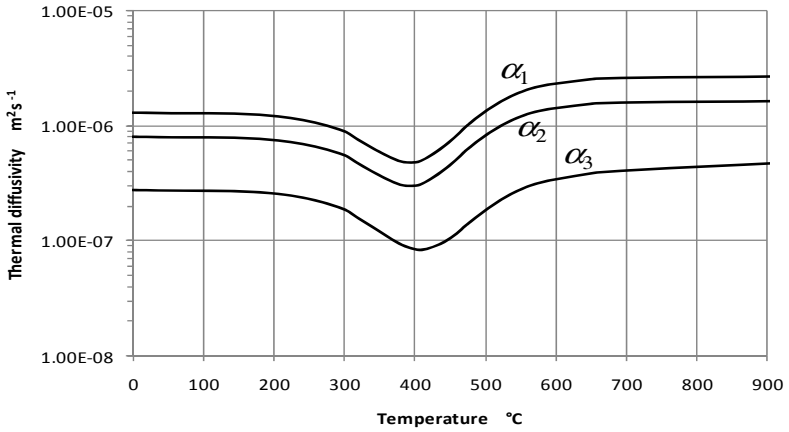

Figure 3. Values of the three principal thermal diffusivities of the CFRP wing box laminate as a function of temperature.

RESULTS AND DISCUSSION

Onset of damage

During the fire exposure tests a near-constant hot face temperature was achieved within 40 seconds of application of the heat flux. This temperature was 750°C in the case of the 75 kWm^{-2} heat flux and 1040°C at 185 kWm^{-2}. The temperatures at the centre of the cold face are shown in Figure 4, along with the values from the ANSYS modelling, which showed good agreement. Figure 5 shows the fire damage that can be seen in the 185 kWm^{-2} after cutting through the centre of the sample. A clearly visible arc-shaped damage region grows to extend well-beyond the mask area, indicating that in-plane heat conduction is significant. After 8 minutes at 185 kWm^{-2} this region extended almost through the full sample thickness at the centre. It can also be seen that the reinforcement in the arc-shaped region is largely depleted of resin, allowing exposed fibres to 'loft'

from the surface. The 75 kWm^{-2} samples showed a much smaller visible damage region, extending roughly 2mm into the thickness.

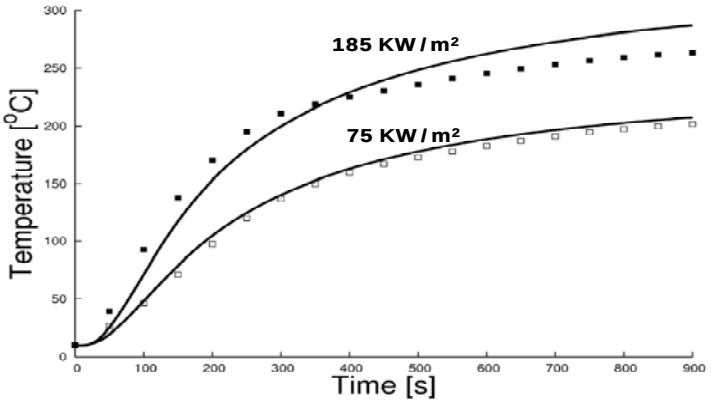

Figure 4. Variation of the cold face temperature during fire exposure (points), along with the modelled temperature variation (continuous line) using ANSYS.

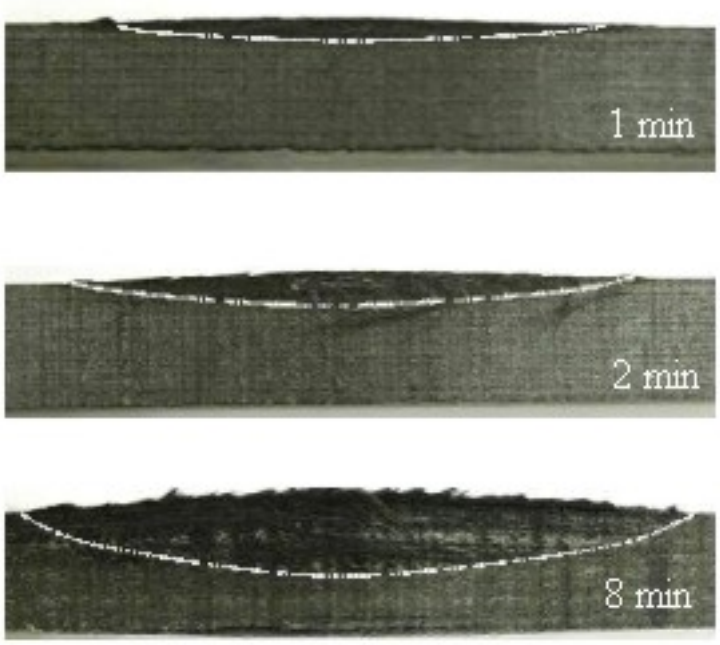

Figure 5. Appearance of the 185 kWm^{-2} samples after various periods of exposure.

Figure 6 shows the results of the ultrasonic time-of-flight characterisation of the sample damage. The greater damage growth in the 185 kWm^{-2} samples is very clear.

Examples of micrographs of polished sections through the centre region are shown in Figure 7. The first damage features that could be seen, furthest from the hot surface, were small delaminations. Nearer to the hot surface, voids and other more obvious

signs of charring could be seen. Finally, in the later stages of exposure to the higher heat flux, fully exposed fibres could be seen close to the exposed face.
The depth of the first damage features was measured using the ultrasonic non-destructive method. Later, after sectioning and polishing, this was measured using microscopy. The two values, which are shown in Figure 8, can be seen to be fairly similar. This confirms that ultrasonic NDE is capable of characterising small delaminations of roughly the same dimensions as can be observed microscopically.

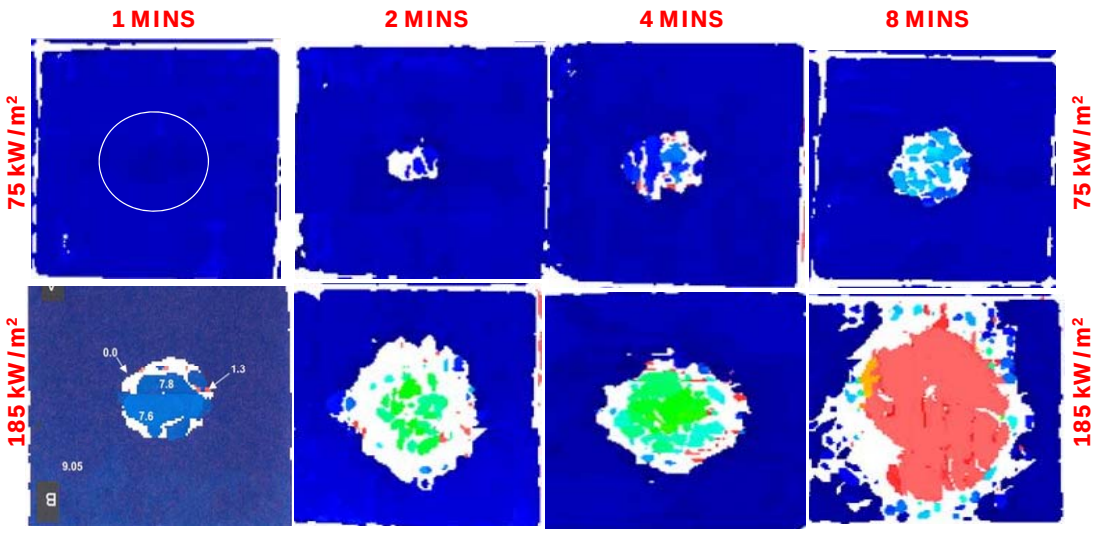

Figure 6. Ultrasonic time-of-flight images of damage at 75 kWm^{-2} and 185 kWm^{-2}, after 1, 2, 4 and 8 minutes. The size of masked region is shown on the first image.

It would be expected that delaminations might commence around the onset of resin decomposition, as measured by TGA, which, at conventional heating rates, is around 350°C. This is over 150°C higher than the resin glass transition temperature, in a region where the resin can be expected to possess very little strength- hence their ease of formation. The question of whether there are any damage processes at temperatures lower than this is still open. Experience with other composite systems suggests that post-curing and cross-linking occur in the region between Tg and decomposition: effects which often have a beneficial effect on mechanical properties. It is also possible however that, prior to decomposition, some damaging chemical changes may occur. Extensive property measurements in this high temperature region would be desirable, to determine whether any damaging changes do take place.

Figure 9 shows the residual compressive strength (ASTM D7137) of the samples following fire exposure. As mentioned this was determined on the damaged laminates using an anti-buckling frame similar to the type employed in compression-after-impact tests. In keeping with the results of the damage measurements the compressive strength falls to about 80% of the undamaged value in the case of the lower heat flux. However, at 185 kWm^{-2} there is a significant and progressive strength loss, down to about 1/3 of the original value. It is interesting to correlate the results of the NDE and optical measurements of damage depth with the residual compressive strength results. The 'two layer' model (REF) has been used successfully in the past to model the residual strength of fire-damaged composite components. This model assumes the damaged

material to comprise two layers: an undamaged layer with virgin properties and a damaged layer, with greatly diminished or near-zero property values.

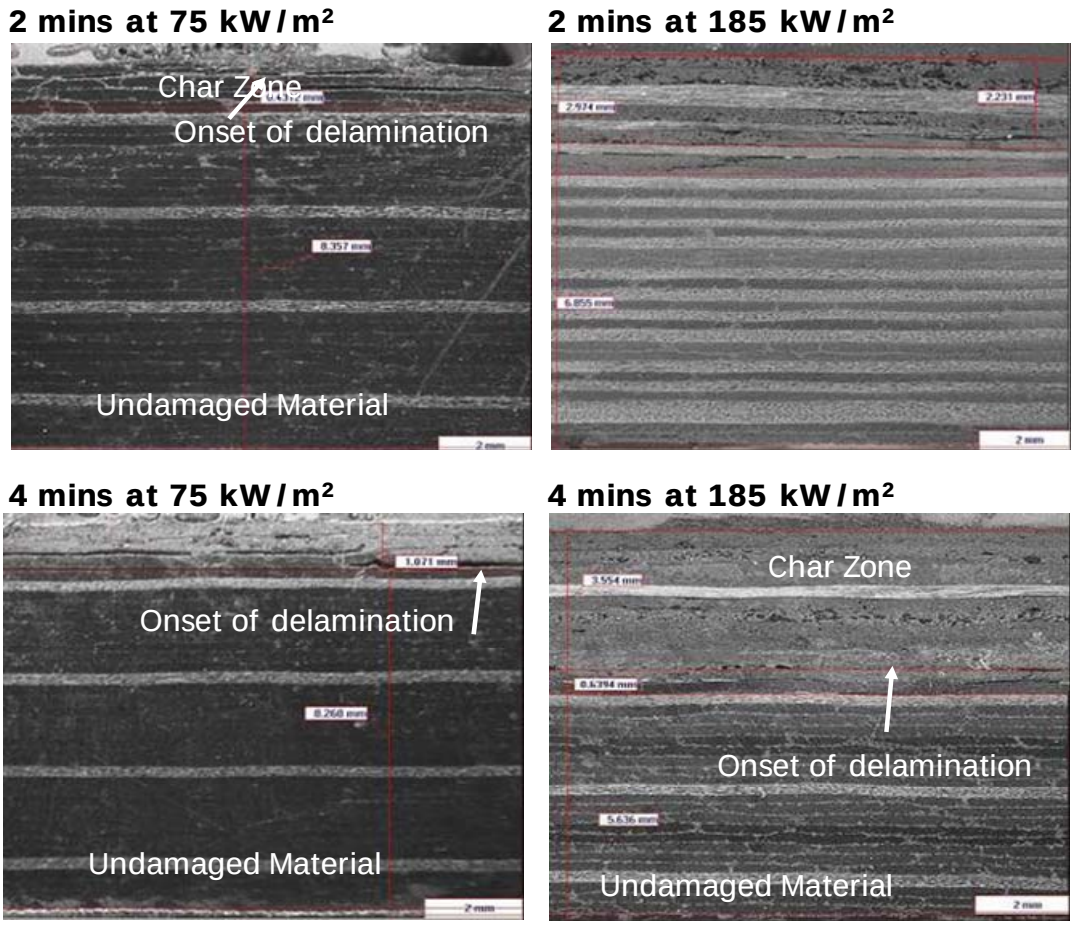

Figure 7. Micrographs of polished sections of specimens at 75 kWm^{-2} and 185 kWm^{-2}, exposed for 2 and 4 minutes.

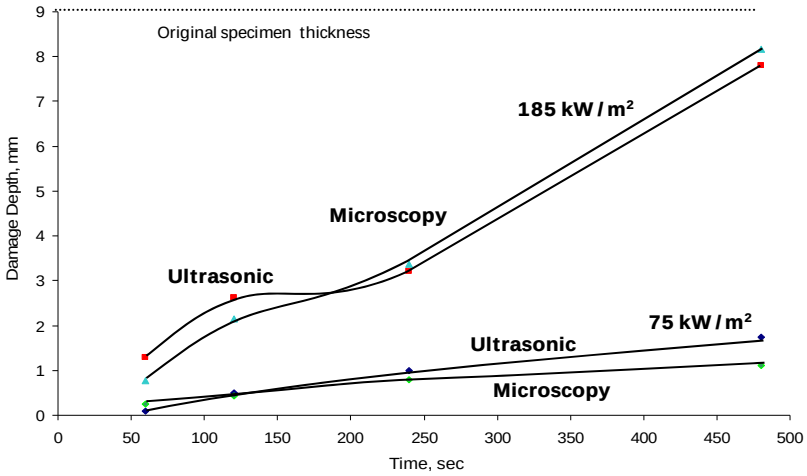

Figure 8. Development of delamination damage at 75 kWm^{-2} and 185 kWm^{-2}, as observed by ultrasonic time-of-flight scan and optical microscopy.

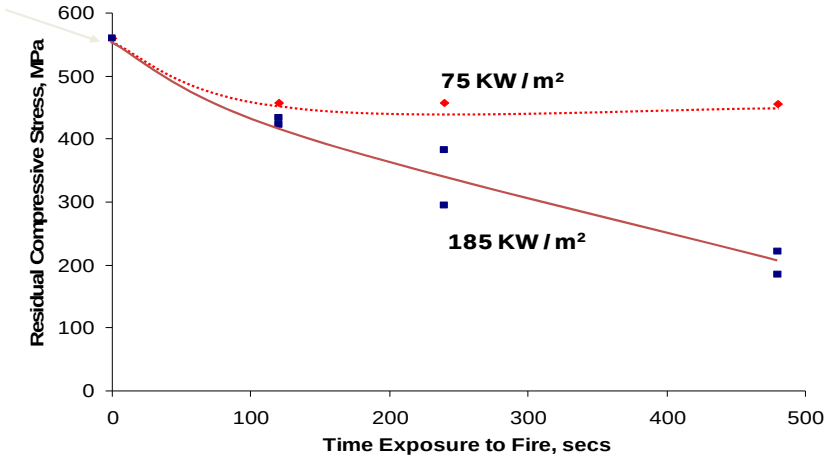

Figure 9. Residual compressive strength of fire-damaged laminates (ASTM D7137) vs. exposure time.

Several undamaged specimens were machined with 40mm (the mask diameter) recesses of different depth. Measuring the residual compressive strength of these samples provided a 'calibration' of strength vs. damage depth, which was used to interpret the results of Figure 9. This assumed the damage region to be circular in shape and of uniform depth with zero residual strength. Given the approximate nature of each of these assumptions, agreement between the damage depth estimate based on compressive strength, and the other measurements is quite good.

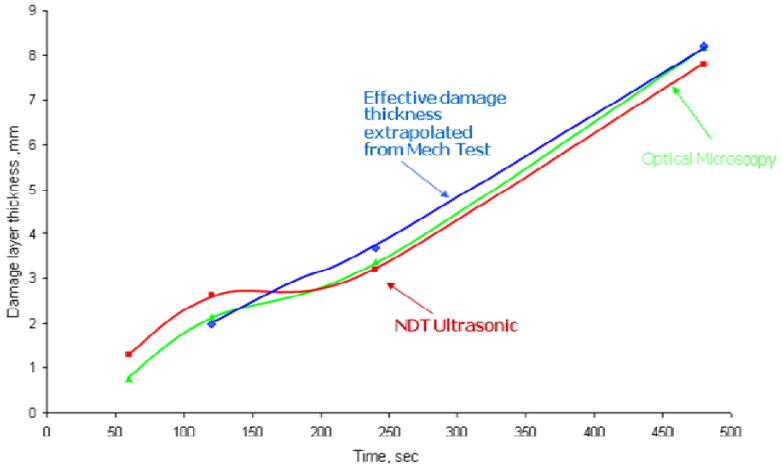

Figure 10. Damage depth at 185 kWm^{-2} estimated from the residual compressive strength test, assuming the 'two layer' model (REF), compared to damage depth from ultrasonic measurements and optical microscopy.

Thermal modelling.

Figure 11 shows the FE modelled temperature field in the CFRP slab at 185 kWm^{-2} after 8 minutes. The temperature rise and thermal damage extend well beyond the edge of the mask region. It can also be seen that the rate of heat propagation in-plane is

much faster than that in the through-thickness direction. The effect of the in-plane thermal anisotropy of the laminate can also be seen. The thermal model was used to derive information about the temperature required for delaminations to occur. Figure 12 shows two estimates for the damage depth for each heat flux. The curves were calculated by assuming damage to occur when the material reaches a particular temperature, in this case 350°C or 420°C.

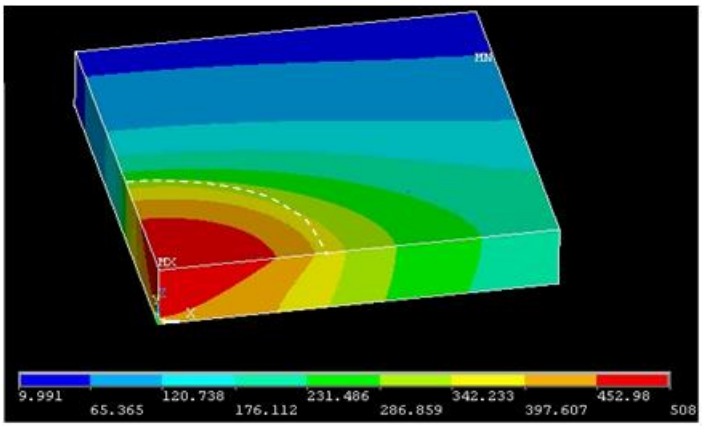

Figure 11. Plot of 3-D temperature distribution within the sample at 185 kWm^{-2} after 8 minutes. The location of the calcium silicate mask is shown.

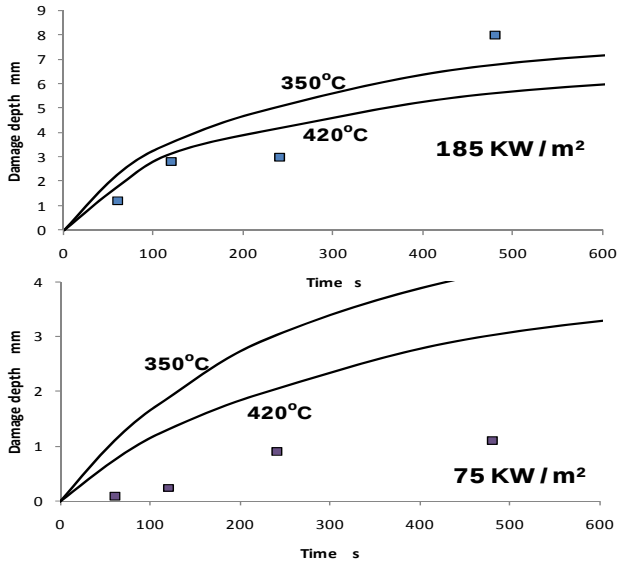

Figure 12. Comparison of damage depth from the thermal model (assuming delamination occurs at 350°C or 420°C) and from the ultrasonic measurements.

These two temperatures correspond roughly to the onset and finish of the resin decomposition process, as determined by TGA. The results from the ultrasonic measurements are also shown for comparison. It can be seen that, for a heat flux of 185 kWm^{-2}, there is reasonable correspondence between the measured and modelled data. However, at the lower heat flux the model appears to predict that the damage onset occurs at an even higher temperature. Further work is needed to clarify what actually

occurs. The discrepancy may be due to the heating rate in the test being approximately an order of magnitude higher than that achievable with TGA. It may also reflect one of the limitations of TGA, namely that the decomposition process in the resin depends to some extent on the constraint offered by the structure of the material around it.

CONCLUSIONS

The tests have shown that delamination damage occurs in CFRP as a result of fire exposure. This damage is detectable by portable ultrasonic equipment. Delaminations occur after the onset of resin decomposition, as measured by TGA, but further work is needed to determine the exact temperature for permanent damage. The onset of delaminations correlates with a reduction in compressive strength, using the 'two layer' model. Temperature dependent thermal properties, including anisotropic values of thermal conductivity, enabled the 3-D temperature field to be modelled using an FE package.

ACKNOWLEDGEMENTS

This project was funded by the European Commission *MOMENTUM* Marie Curie Research Training Network, contract No. MRTN-CT-2005-019198.

References

1. J.B. Henderson, J.A. Wiebelt and M.R. Tant. A model for the thermal response of polymer composite materials with experimental verification. *Journal of Composite Materials*, 1985;19: 579-595.
2. A.P. Mouritz and A.G. Gibson, Fire Properties of Polymer Composite Materials, Springer, Dordrecht, 2006.
3. V. Urso-Miano and A.G. Gibson, Fire model for FRP using apparent thermal diffusivity (ATD), *Plastics, Rubber and Composites*, 2009, 6, 87-92.
4. A.G. Gibson, P.H.N. Wright, Y.-S. Wu, A.P. Mouritz, Z. Mathys and C.P. Gardiner, *Plastics, Rubbers & Composites*, 2003; 32,81-90.
5. A.G. Gibson, Y.-S. Wu, J.T. Evans, J.T. and A.P. Mouritz, *Journal of Composite Materials*, **40**, (2006), 639-658.
6. S. Feih, Z. Mathys, A.G. Gibson and A.P. Mouritz, *Composites Science & Technology*, **67**, (2007), 551-564.
7. J. Lua, J. O'Brien, C.T. Key, Y. Wu and B.Y. Lattimer, *Composites*, 37A, (2006), 1024-1039.
8. Feih, S., Mouritz, A.P., Mathys, Z. and Gibson, A.G., *J. of Comp. Materials*, **41**, (2007), 2387-2410.
9. H.L. McManus. Prediction of fire damage to composite aircraft structures. *Proceedings of the 9th Int. Conf. on Composite Materials*, Madrid, Spain, July 1993, pp. 929-936.
10. P.G.B. Seggewiss, Properties of fire-damaged polymer matrix composites, *Proceedings of the 3rd Int. Conf. on Composites in Fire*, University of Newcastle, 9-10 Sept., 2003.
11. S. Yarlagadda, A. Chatterjee, J. W. Gillespie Jr., Jennifer C. Kiel, Doug S. Dierdorf: 'Post-Fire Damage Assessment of a Composite Wing-box' Air Force Research Lab Tyndall, Report A033424, May 2004.